FRACTURE OF PIEZOELECTRIC MATERIALS

Tong-Yi Zhang* and Minghao Zhao

Department of Mechanical Engineering, Hong Kong University of Science and Technology
Clear Water Bay, Kowloon, Hong Kong, China, * E-mail: mezhangt@ust.hk

ABSTRACT

The present work studies, theoretically and experimentally, the fracture behavior of piezoelectric ceramics. For an electrically insulating crack, the ratio of α/β plays an important role in the energy release rate, where α is the ratio of the minor semi-axis, *b,* to the major semi-axis, *a,* of the ellipse, and β is the ratio of the dielectric constant of the cavity to the effective dielectric constant of the material. There are three limiting values in the energy release rate, respectively corresponding to $\alpha/\beta \to 0$ for an electrically permeable crack, $\alpha/\beta \to$ a finite nonzero value for general cases and $\alpha/\beta \to \infty$ for an electrically impermeable crack. For an electrically conductive crack, the applied electric field parallel to the crack drives the crack to propagate. When electric yield occurs at a crack tip, the global energy release rate is the same as that derived from linear fracture mechanics, while the local energy release rate shows a linear relationship between the fracture toughness and the applied electric field. The experimental results illustrate that for PZT-841 and PZT-4 ceramics, the degree of scattering of measured data was considerably enhanced by an applied electric field. Either a positive or a negative electric field reduced the fracture toughness. The experimental results also confirmed that there exist mechanical- and electrical-fracture toughness for PZT-4 ceramics and both are material properties. The mechanically- and electrically- critical energy release rates are, respectively, 8.7(±1.1) and 223.7(±45.5) N/m.

KEYWORDS

piezoelectric medium, crack, energy release rate, fracture toughness, polarization saturation

INTRODUCTION

Along with the application of piezoelectric materials in more and more sophisticated structures, their mechanical reliability becomes increasingly important. Thus, many efforts have being made to study the fracture behavior of those materials [1-23]. One of the most interesting aspects is about the effect of electric field on the fracture behavior. Many experimental results are inconsistent or even contradicted, which makes the study of fracture of piezoelectric ceramics more challenging. The present work briefly summarizes the work done at the Hong Kong University of Science and Technology, on this topic.

TWO-DIMENSIONAL SOLUTION

Figure 1 shows schematically a crack of length 2*a* in an infinite piezoelectric medium under remotely

uniform electrical loads and in-plane and anti-plane mechanical loads. Using Stroh's formalism [1-3], the general two-dimensional solution can be written in the form

$$\begin{aligned} &\mathbf{u} = \mathbf{A}\mathbf{f} + \overline{\mathbf{A}\mathbf{f}}, \quad \boldsymbol{\psi} = \mathbf{L}\mathbf{f} + \overline{\mathbf{L}\mathbf{f}}, \quad \boldsymbol{\Sigma}_2 = \boldsymbol{\psi}_{,1}, \quad \boldsymbol{\Sigma}_1 = -\boldsymbol{\psi}_{,2}, \\ &\mathbf{u} = \begin{pmatrix} u_1 & u_2 & u_3 & \varphi \end{pmatrix}^{\mathrm{T}}, \quad \boldsymbol{\Sigma}_1 = \begin{pmatrix} \sigma_{11} & \sigma_{21} & \sigma_{31} & D_1 \end{pmatrix}^{\mathrm{T}}, \quad \boldsymbol{\Sigma}_2 = \begin{pmatrix} \sigma_{12} & \sigma_{22} & \sigma_{32} & D_2 \end{pmatrix}^{\mathrm{T}}, \end{aligned} \tag{1}$$

where $u_i, \varphi, \sigma_{ij}$ and D_i are the displacements, electric potential, stresses and electric displacements, respectively. The two 4×4 matrixes, **A** and **L,** are related to the material properties, with A_{ij} and L_{ij} denoting their elements, repectively. The analytical function vector, $\mathbf{f}(z) = \begin{pmatrix} f_1(z_1) & f_2(z_2) & f_3(z_3) & f_4(z_4) \end{pmatrix}^{\mathrm{T}}$, is determined by the remote loads and the boundary conditions.

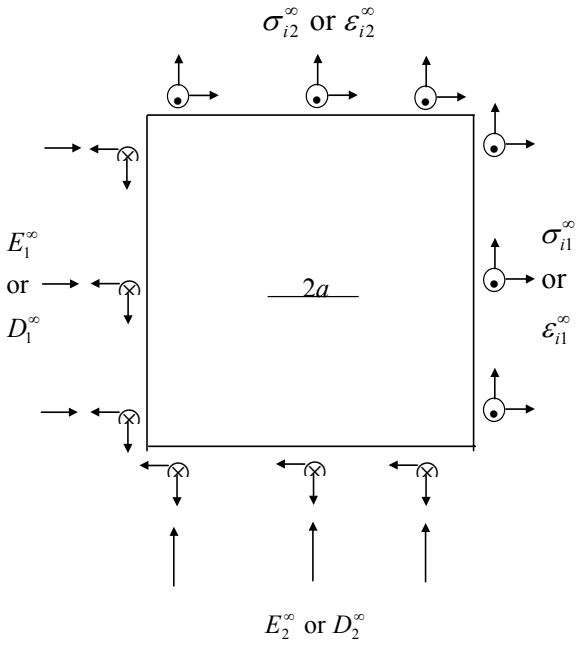

Fig. 1 A crack in an infinite piezoelectric medium under combined remote loadings.

INSULATING CRACK

Zhang *et al*. [3] obtained the solutions for an insulating elliptical cavity using the exact boundary conditions, traction-free, surface charge-free and continuity of electric potential, along the cavity surface. The results depend greatly on the ratio of α/β, where α is the ratio of the minor semi-axis, *b,* to the major semi-axis, *a,* of the ellipse, and β is the ratio of the dielectric constant of the cavity to the effective dielectric constant of the piezoelectric material. When the cavity shrinks into a slit crack, there are three limiting cases, respectively corresponding to $\alpha/\beta \to 0$ for an electrically permeable crack, $\alpha/\beta \to$ a finite nonzero value for general cases and $\alpha/\beta \to \infty$ for an electrically impermeable crack. Only the two cases of electrically permeable and impermeable cracks are discussed in the present paper. From these solutions, the energy release rate for the two cases can be expressed in terms of the intensity factors at the crack tip

$$J = \frac{\mathbf{K}^{\mathrm{T}}\left(\mathbf{B} + \overline{\mathbf{B}}\right)\mathbf{K}}{4}, \tag{2}$$

where $\mathbf{K} = \begin{pmatrix} K_{\mathrm{II}} & K_{\mathrm{I}} & K_{\mathrm{III}} & K_D \end{pmatrix}^{\mathrm{T}}$ with the components being the stress intensity factors of the three modes, K_{I}, K_{II} and K_{III}, and the electric displacement intensity factor, K_D, respectively. **B** is a Hermitian matrix,

$$\mathbf{B} = i\mathbf{A}\mathbf{L}^{-1} = \begin{pmatrix} \mathbf{B}_1 & \mathbf{B}_2 \\ \mathbf{B}_3 & B_{44} \end{pmatrix}, \tag{3}$$

The upper left-hand block $\mathbf{B}_1$ is a 3×3 matrix and the lower right-hand element B_{44} is scalar. For stable materials, **B** has the following properties [1, 2]

$$\mathbf{B}_2 = \overline{\mathbf{B}}_3^{\mathrm{T}}, \quad B_{44} < 0\,. \tag{4}$$

Electrically permeable crack

The electrically permeable boundary conditions correspond to $\alpha/\beta \to 0$ and lead to the intensity factors

$$K_{\mathrm{I}} = \sqrt{\pi a}\,\sigma_{22}^{\infty}, \quad K_{\mathrm{II}} = \sqrt{\pi a}\,\sigma_{12}^{\infty}, \quad K_{\mathrm{III}} = \sqrt{\pi a}\,\sigma_{32}^{\infty},$$
$$K_D = -\frac{\sqrt{\pi a}}{2B_{44}}\left[\left(B_{41}+\overline{B_{41}}\right)\sigma_{12}^{\infty} + \left(B_{42}+\overline{B_{42}}\right)\sigma_{22}^{\infty} + \left(B_{43}+\overline{B_{43}}\right)\sigma_{32}^{\infty}\right] \tag{5}$$

Equation (5) shows that the electric displacement intensity factor is completely induced by the piezoelectric effect rather than by the applied electric loads. Then, substituting Eq. (5) into Eq. (2), we see that the energy release rate is independent of the applied electric field either perpendicular or parallel to the crack. In other words, the energy release rate has nothing to do with the applied electric fields.

Electrically impermeable crack

An electrically impermeable crack ignores the electric field within the crack. Thus, the intensity factors are given by

$$\left(K_{\mathrm{II}} \quad K_{\mathrm{I}} \quad K_{\mathrm{III}} \quad K_D\right) = \left(\sqrt{\pi a}\,\sigma_{12}^{\infty} \quad \sqrt{\pi a}\,\sigma_{22}^{\infty} \quad \sqrt{\pi a}\,\sigma_{32}^{\infty} \quad \sqrt{\pi a}\,D_2^{\infty}\right). \tag{6}$$

Equations (2) and (6) show that the remote mechanical loads, $\sigma_{12}^{\infty}, \sigma_{22}^{\infty}$ and σ_{32}^{∞}, as well as the electrical load, D_2^{∞}, determine the energy release rate, while the applied electric field parallel to the crack contributes nothing to the energy release rate. Furthermore, we can easily see that the applied electric field perpendicular to the crack impedes the crack propagation because B_{44} is negative as given in Eq. (4).

CONDUCTING CRACK

If the crack is electrically conducting, the boundary conditions along crack faces are traction-free and constant electric potential. For simplicity, it is assumed that there are no net electric charges on the crack faces and the constant electric potential on the crack faces is zero. Then, the intensity factors take the form of

$$K_{\mathrm{I}} = \sqrt{\pi a}\,\sigma_{22}^{\infty}, \quad K_{\mathrm{II}} = \sqrt{\pi a}\,\sigma_{12}^{\infty}, \quad K_{\mathrm{III}} = \sqrt{\pi a}\,\sigma_{32}^{\infty}, \quad K_{E_1} = \sqrt{\pi a}\,E_1^{\infty}. \tag{7}$$

The energy release rate is expressed in terms of the intensity factors

$$J = \left(K_{\mathrm{II}} \quad K_{\mathrm{I}} \quad K_{\mathrm{III}} \quad -K_{E_1}\right)\frac{i\left[\mathbf{P}\mathbf{Q}^{-1} - \overline{\mathbf{P}\mathbf{Q}^{-1}}\right]}{4}\begin{pmatrix} K_{\mathrm{II}} \\ K_{\mathrm{I}} \\ K_{\mathrm{III}} \\ -K_{E_1} \end{pmatrix}, \tag{8}$$

where $i = \sqrt{-1}$, and

$$\mathbf{Q} = \begin{pmatrix} L_{11} & L_{12} & L_{13} & L_{14} \\ L_{21} & L_{22} & L_{23} & L_{24} \\ L_{31} & L_{32} & L_{33} & L_{34} \\ A_{41} & A_{42} & A_{43} & A_{44} \end{pmatrix}, \quad \mathbf{P} = \begin{pmatrix} A_{11} & A_{12} & A_{13} & A_{14} \\ A_{21} & A_{22} & A_{23} & A_{24} \\ A_{31} & A_{32} & A_{33} & A_{34} \\ L_{41} & L_{42} & L_{43} & L_{44} \end{pmatrix}. \tag{9}$$

Equation (8) shows that only the electric field parallel to the crack affects the crack propagation. We explicitly demonstrate this result with a mode III conductive crack. When the poling direction of a transversely isotropic piezoelectric medium is perpendicular to the crack, the anti-plane deformation decoupled from the in-plane deformation and the intensity factors for a mode III conductive crack are given by

$$K_{\mathrm{III}} = \sqrt{\pi a}\sigma_{32}^{\infty}, \quad K_{E_1} = \sqrt{\pi a}E_1^{\infty}. \tag{10}$$

Consequently, the energy release rate for the mode III conductive crack is

$$J = \frac{\pi a}{2}\left[\frac{1}{c_{44}}\left(\sigma_{32}^{\infty}\right)^2 + \left(\kappa_{11} + \frac{e_{15}^2}{c_{44}}\right)\left(E_1^{\infty}\right)^2\right]. \tag{11}$$

Equation (11) shows clearly that the applied electric field parallel to the crack drives the crack to propagate.

POLARAZATION SATURATION MODEL

For an electrically impermeable crack, Gao *et al*. [4] proposed a strip polarization model to examine the electrical yielding effect on the fracture behavior of electrically insulating cracks. In this model, piezoelectric ceramics are treated as mechanically brittle and electrically ductile materials. The electrical saturation is analogous to the classical Dugdale model. To emphasize the physical insight, Gao *et al*. [4] considered a simplified piezoelectric material to make the derivation process straightforward. In the present work, the complete governing equations are used. The local intensity factors are the sum of the intensity factors induced by the applied field and the saturation zone

$$\mathbf{K}^{l} = \mathbf{K}^{a} + \mathbf{K}^{d}, \tag{12}$$

where the applied intensity factor vector $\mathbf{K}^{a}$ is given in Eq. (6) and the intensity factor vector $\mathbf{K}^{d}$ caused by the polarization zone takes the form of

$$\left(K_{\mathrm{II}}^{l} \quad K_{\mathrm{I}}^{l} \quad K_{\mathrm{III}}^{l} \quad K_{D}^{l}\right) = \left(K_{\mathrm{II}}^{a} - \frac{\mathbf{L}_1\mathbf{L}_4^{\mathrm{T}}}{\mathbf{L}_4\mathbf{L}_4^{\mathrm{T}}}K_{D}^{a} \quad K_{\mathrm{I}}^{a} - \frac{\mathbf{L}_2\mathbf{L}_4^{\mathrm{T}}}{\mathbf{L}_4\mathbf{L}_4^{\mathrm{T}}}K_{D}^{a} \quad K_{\mathrm{III}}^{a} - \frac{\mathbf{L}_3\mathbf{L}_4^{\mathrm{T}}}{\mathbf{L}_4\mathbf{L}_4^{\mathrm{T}}}K_{D}^{a} \quad 0\right). \tag{13}$$

As a result, the local energy release rate is given by

$$J^{l} = \left(K_{\mathrm{II}}^{a} - \frac{\mathbf{L}_1\mathbf{L}_4^{\mathrm{T}}}{\mathbf{L}_4\mathbf{L}_4^{\mathrm{T}}}K_{D}^{a} \quad K_{\mathrm{I}}^{a} - \frac{\mathbf{L}_2\mathbf{L}_4^{\mathrm{T}}}{\mathbf{L}_4\mathbf{L}_4^{\mathrm{T}}}K_{D}^{a} \quad K_{\mathrm{III}}^{a} - \frac{\mathbf{L}_3\mathbf{L}_4^{\mathrm{T}}}{\mathbf{L}_4\mathbf{L}_4^{\mathrm{T}}}K_{D}^{a}\right)\frac{(\mathbf{B}_1 + \overline{\mathbf{B}_1})}{4}\begin{pmatrix} K_{\mathrm{II}}^{a} - \frac{\mathbf{L}_1\mathbf{L}_4^{\mathrm{T}}}{\mathbf{L}_4\mathbf{L}_4^{\mathrm{T}}}K_{D}^{a} \\ K_{\mathrm{I}}^{a} - \frac{\mathbf{L}_2\mathbf{L}_4^{\mathrm{T}}}{\mathbf{L}_4\mathbf{L}_4^{\mathrm{T}}}K_{D}^{a} \\ K_{\mathrm{III}}^{a} - \frac{\mathbf{L}_3\mathbf{L}_4^{\mathrm{T}}}{\mathbf{L}_4\mathbf{L}_4^{\mathrm{T}}}K_{D}^{a} \end{pmatrix}. \tag{14}$$

Because the polarization zone shields the crack tip electrically and completely, the local electrical displacement intensity factor is zero. The applied electric field contributes to the local energy release rate via the piezoelectric effect. The local energy release rate, as a failure criterion, yields a linear relationship between the applied mechanical load and electric field. But the global energy release rate is the same as that from linear fracture mechanics, which predicts that either a positive or negative electric field impedes the crack propagation.

EXPERIMENTAL RESULTS

Fracture test

Compact Tension (CT) tests and Indentation Fracture (IF) tests were carried out on PZT-841 ceramics under an applied electric field. The material is poled PZT-841 with an average grain size of 4-5 μm. The composition of PZT-841 is near, but in the tetragonal side of the morphotropic phase boundary. In the CT tests, the notch on each sample was cut using a diamond saw with a 0.2 mm-thick blade and the notch tip

was further sharpened with a wire saw of 0.05 mm in diameter. The poling direction was perpendicular to the notch. About 10 samples were tested at each level of the electric fields, except that 33 samples were tested at the electric field of 15 kV/cm to study the distribution of fracture toughness. The energy release rate was calculated by the finite element method and then converted into the mode I stress intensity factor. In the IF tests, the load was 49.0 N and the electric field of 4 kV/cm was applied either parallel or antiparallel to the poling direction of the sample. Under each level of the electric fields, about 10 indentations were performed. Only the fracture behavior of the cracks perpendicular to the poling direction is reported in this paper. Figures 2(a) and 2(b) show the variation of K_{IC} with the applied electric field obtained from the CT and IF tests, respectively. Under purely mechanical loading, the averaged K_{IC}s are $1.12 \pm 0.05 MPa\sqrt{m}$ and $1.01 \pm 0.06 MPa\sqrt{m}$, respectively, from the two methods. The mean value of K_{IC} is reduced by either a positive or a negative applied electric field in both types of testing. In the CT tests, the negative field of 7.5 kV/cm reduces the averaged K_{IC} by $0.25 MPa\sqrt{m}$, while the same strength positive field reduces the averaged K_{IC} by $0.10 MPa\sqrt{m}$. Similarly, in the IF tests, a reduction of $0.21 MPa\sqrt{m}$ or $0.10 MPa\sqrt{m}$ results from the application of a negative or positive field of 4 kV/cm. These facts indicate that a negative field has a stronger influence on the averaged K_{IC} than a positive field does. Applying a positive electric field of 15 kV/cm reduces further the averaged K_{IC} to $0.92 \pm 0.14 MPa\sqrt{m}$ in the CT tests, resulting in a relative reduction of 18%.

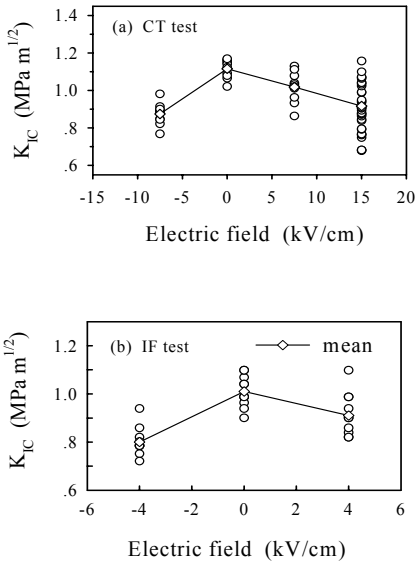

Fig. 2 Effect of an electric field on the fracture toughness.

Conducting crack

CT samples used in this study were made from poled PZT-4 piezoelectric ceramics and the poling direction was parallel to the notch. A 0.25 mm wide notch in every sample was cut and its tip was sharpened further by a wire saw of radius 0.1 mm. Silver paint was filled into the notch to make it function as an electrode. Thus, the crack becomes electrically conducting. Two loading types were applied in this study. One is purely mechanical loading and the other is purely electric loading. In the electric loading tests, a static voltage was applied to a sample at the electrodes and increased until the sample was failed. All tests were carried out at room temperature and 30 samples were tested for each loading type. It was observed that electrical breakdown was usually accompanied by fracture. The fracture surfaces are flat for samples fractured under mechanical loads. A critical voltage causes dielectric breakdown tunnel and rough fracture surfaces. The finite element method was used to calculate the energy release rate for the given samples. The critical energy release rate under mechanical loading was calculated from the fracture load and the corresponding ligament, as shown in Fig. 3(a). The mean of the mechanical critical energy release rate is G_{IC}^{M} =8.7±0.4 N/m. It is clearly seen that the linear regression of the plot is very close to a horizontal line, indicating that the critical energy release rate is a material constant independent on the sample ligament. Similarly, the critical energy release rate under electric loading was calculated from the critical voltage and the ligament. Figure 3(b) presents the electrical critical energy release rate versus sample ligament. The linear regression of the plot is also almost a horizontal line. This fact, in analogy with the mechanical loading situation, means that the

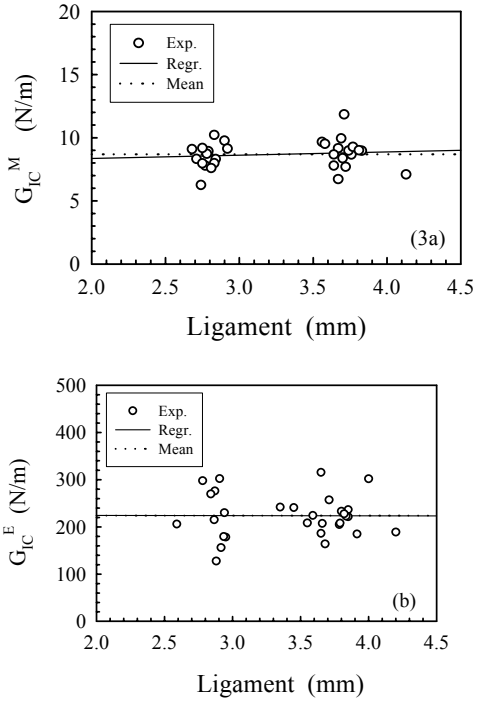

Fig. 3 The energy release rate versus the ligament, (a) mechanical loading and (b) electrical loading.

electrical critical energy release rate is a material property with the value G_{IC}^{E}=223.7±17.0 N/m for PZT-4 ceramics. The significance of the existence of G_{IC}^{E} is that it enables fracture mechanics concepts to be used in understanding dielectric failure, and it provides a useful material property for designers of electronic and electromechanical devices.

CONCLUDING REMARKS

The linear theoretical results show that the electric field has different effects on the energy release rate for different types of cracks. The energy release rate is independent of the applied electric field for electrically permeable cracks. The applied electric field perpendicular to an impermeable crack impedes the crack to propagate, while the applied electric field parallel to a conducting crack drives the crack to propagate. However, the strip polarization saturation model, when electrical yield occurs in front of the crack tip, predicts that the propagation of an impermeable crack is driven by a perpendicular positive electric field and impeded by a perpendicular negative electric field.

The experimental results of both compact tension tests and indentation fracture tests show that either a positive or negative electric field perpendicular to the electrically insulating crack always assists the applied mechanical loads to fracture the sample. For electrically conductive cracks, there is a critical energy release rate under purely electrical loading, just like the case under purely mechanical loading. In terms of the energy release rate, however, the electrical fracture toughness is about 25 times higher than the mechanical fracture toughness.

ACKNOWLEDGEMENTS: This work is supported by a grant from the Research Grant Council of the Hong Kong Special Administrative Region, China.

REFERENCES

1. Barnett, D. M. and Lothe, J. (1975) *Phys. Stat. Sol.* (*b*) **67**, 105.
2. Suo, Z., Kuo, C. M., Barnett, D. M. and Willis, J. R. (1992) *J. Mech. Phys. Solids* **40**, 739.
3. Zhang, T.-Y., Qian, C.-F. and Tong, P. (1998) *Int. J. Solids Structures* **35**, 2121.
4. Gao, H., Zhang, T.-Y. and Tong, P. (1997) *J. Mech. Phys. Solids* **45**, 491.
5. Cao, H. and Evans, A. G. (1993) *J. Am. Ceram. Soc*. **76**, 890.
6. Cherepanov, G. P. (1979). *Mechanics of Brittle Fracture*, McGraw-Hill, New York.
7. Deeg, W.F.J. (1980). The analysis of dislocation, crack, and inclusion problems in piezoelectric solids. *PhD Thesis*, Stanford University.
8. Fu, R. and Zhang, T.-Y. (1998). *J. Am. Ceram. Soc.* **81**, 1058.
9. Fu, R., Qian, C.-F. and Zhang, T.-Y.(2000) *Appl. Phys. Letters*, **76**, 126.
10. Zhang, T.-Y. and Hack, J. E. (1992) *J. Appl. Phys*. **71**, 5865.
11. Zhang, T.-Y.(1994) *Int. J. Fracture* **68**, R33.
12. Zhang, T.-Y. and Tong, P. (1996) *Int. J. Solids Structures* **33**, 343.
13. Lynch, C.S. (1996) *Acta Mater*. **44**, 4137.
14. McMeeking, R. M. (1989) *J. Appl. Math. Phys.* **40**, 615.
15. Mehta, K. and Virkar, A.V. (1990) *J. Am. Ceram. Soc.*, **73**, 567.
16. Pak, Y.E. (1990) *J. Appl. Mech.,* **57**, 647.
17. Sosa, H. and Pak, Y. E. (1990) *Int. J. Solids Structures* **26**, 1.
18. Sosa, H. (1992) *Int. J. Solids Structures* **29**, 2613.
19. Suo, Z. (1993) *J. Mech. Phys. Solids* **41**, 1155.
20. Zhu, T. and Yang, W.(1999) *J. Mech. Phys. Solids*, **47**, 81.
21. Qin, Q. H., Mai, Y. W. and Yu, S. W. (1999) *Int. J. Solids Structures* **36**, 427.
22. Kogan, L., Hui, C. Y. and Molkov V. (1996) *Int. J. Solids Struct.* **33**, 2719.
23. Zhang, T.-Y., Zhao, M. H. and Tong, P. (2001) Fracture of Piezoelectric Ceramics, *Advances in Applied Mechanics*, in press.